Structure and energetics of Cu_N clusters with $(2 \leqslant N \leqslant 150)$: An embedded-atom-method study

Valeri G. Grigoryan,* Denitsa Alamanova,† and Michael Springborg‡
Physical and Theoretical Chemistry, University of Saarland, 66123 Saarbrücken, Germany
(Received 29 August 2005; revised manuscript received 21 November 2005; published 15 March 2006)

We use the embedded-atom method (EAM) in the version of Daw, Baskes, and Foiles (DBF) to determine the three most stable isomers of Cu_N clusters with N from 2 to 150. Randomly generated initial configurations are optimized with the *variable metric/quasi-Newton* method combined with our own *Aufbau/Abbau* algorithm for searching the global minima. A detailed comparison is made for clusters with up to 60 atoms obtained with the DBF and the Voter-Chen (VC) versions of the EAM, the many-body Gupta, and the Sutton-Chen 9-6 potentials. Although the two EAM potentials have completely different parametrizations, they yield clusters that are structurally and energetically almost identical. On the other hand, the Sutton-Chen potential strongly overestimates the binding energy of the dimer and the small copper clusters with up to 15 atoms, and therefore, yields clusters with shorter bond lengths. For DBF clusters with up to 150 atoms we analyze many structural and energetic properties such as the overall shape, the construction of atomic shells, the similarity of the clusters with fragments of the fcc crystal or of a large icosahedral cluster, and whether the N-atom cluster resembles the $(N-1)$-atom one with an extra atom added. The most stable clusters have high symmetry, such as the magic-sized Cu_{55} and Cu_{147} that are the second and third Mackay icosahedra, where the latter was obtained for the first time in a completely unbiased structure optimization. The cluster growth is predominantly icosahedral, with islands of fcc, tetrahedral, and decahedral growth.

DOI: 10.1103/PhysRevB.73.115415 PACS number(s): 61.46.Bc, 36.40.−c, 68.65.−k

I. INTRODUCTION

During the past two decades, metal clusters have been an object of extensive theoretical and experimental investigations, due to their unique physical and chemical properties determined by their restricted size. Such particles consist of 10–10 000 atoms and have optical and magnetic properties sensitive to the number of atoms, which makes them useful for nanoscopic devices, drugs, and catalysts. Of particular interest are the so-called *magic-numbered* clusters that possess closed electronic and/or geometric shells which grant them unusual stability. Such clusters have been found for $N=13,38,55,75,147,309,\ldots$ with N being the number of atoms.

Although there are many experimental[1,2] and theoretical[3–8] investigations on copper clusters grown on substrates, and various microscopic as well as spectroscopic studies on free copper clusters[9–11] and on crystalline surfaces,[12–18] even in the most recent experiments[19–23] it has not been possible to determine the structures of the smallest clusters. A useful approach is, therefore, to study these particles with accurate theoretical methods that allow unbiased determination of the structure of clusters with a not too small number of atoms.[24] Unfortunately, with first-principles methods, one is limited to either treat small systems or to make more or less severe assumptions on the structure of the system. On the other hand, with (semi)empirical methods, one can optimize the structure of clusters with even a few thousands of atoms.

During the last ten years, many parameter-free studies on small copper clusters have been published. These include the density-functional study on small neutral and charged copper clusters with up to 7 atoms by Massobrio *et al.*,[25] and the similar work by Calaminici *et al.*[26] on neutral and charged clusters with up to 5 atoms, as well as others based on either *ab initio*[27] or density-functional[28,29] approaches. Olviedo and Palmer[30] studied the Cu_{13}, Ag_{13}, and Au_{13} clusters using a density-functional method with plane-wave basis sets and pseudopotentials implemented in the program VASP. They found that the icosahedron was more stable than the cuboctahedron by 29 meV/atom, but lying with 71 meV/atom above a disordered total-energy minimum. Disordered minimum (C_s) for Cu_{20} was found by Wang *et al.*[31] on the basis of the GGA approximation, in contrast to the tetrahedral Ag_{20} and Au_{20} clusters.

Calculations on larger clusters can be performed only by using semiempirical potentials like the Sutton-Chen,[32] the many-body Gupta,[33] the Finnis-Sinclair,[34] the embedded-atom,[35–39] and related methods,[40–42] and/or molecular-dynamics simulations.[43–47] Using a Monte Carlo minimization approach Doye and Wales[32] determined the global minima for metal clusters with up to 80 atoms modeled by the Sutton-Chen family of potentials.[48] Darby *et al.*[33] studied copper clusters with up to 56 atoms with the many-body Gupta potential.[49] Zhurkin and co-workers[43] studied the structural and thermodynamic properties of copper clusters by means of molecular dynamics and Metropolis Monte Carlo sampling in the so-called transmutational ensemble. Using the Finnis-Sinclair many-body potential[34] Zhang and colleagues[44] simulated melting of a system consisting of 500 copper atoms. The energetics of nanoclusters for five different metals (Ag, Cu, Au, Pd, and Pt) were investigated by Baletto *et al.*[45] by means of quenched molecular dynamics simulations. They considered three structural motifs: Icosahedra (I_h), decahedra (D_h), and truncated octahedra (TO). Scherbarchov and Hendy[47] investigated the static and dynamic coexistence between solid and liquid phases in large silver, copper, and nickel clusters. They found static coexistence in the 561-atom copper and corresponding silver icosa-

hedra, and the 923-atom nickel icosahedron, but not in smaller clusters. Not too small copper clusters ($3 \leqslant N \leqslant 55$) were investigated by Kabir and co-workers[39] using a tight-binding molecular dynamics method. Finally, García-Rodeja and co-workers[35] used the Voter-Chen version of the embedded-atom method to perform molecular dynamics simulations on Ni, Pd, Pt, Cu, Ag, and Au clusters in the size range $N=2-23$.

Although copper does constitute one of the more studied elements in the field of cluster science, this discussion shows that except for the absolutely smallest clusters, all theoretical studies of the structure of Cu clusters, that do not make strong assumptions on the structure, are based on more or less accurate approximate potentials. It is, accordingly, not clear how these potentials will influence the results. In order to address this issue and to obtain a systematic and detailed description of copper clusters over a larger size range, we have performed unbiased structure optimizations on copper clusters Cu_N with N up to 150 atoms. For $N \leqslant 60$ we have compared the results based on four different potentials, whereas for the larger values of N we have used only one potential. Through this detailed study we are able to estimate the limitations and possibilities of the various approaches. Moreover, what maybe is most important, we have systematically studied larger clusters than any earlier study and through carefully constructed descriptors we shall analyze and depict the size-development of various properties of the copper clusters. In addition, we have determined not only the single most stable isomer but the three energetically lowest-lying ones for each cluster size.

The paper is organized as follows. In Sec. II we briefly outline our computational methods, and in Sec. III we present the main results. A brief summary is offered in Sec. IV.

II. COMPUTATIONAL METHODS

Two ingredients are needed in order to determine the properties of the Cu clusters as a function of the size: A method that gives the total energy for a given structure, and a method that is able to locate the structures of the lowest total energy, in particular the global total-energy minimum. For the former we use the embedded-atom method and for the latter our own *Aufbau/Abbau* method. These shall be described briefly below.

A. The total energy

For most of the studies we shall apply the embedded-atom method (EAM) as originally proposed by Daw, Baskes, and Foiles,[50–52] and the version developed later by Voter and Chen.[53–55] The accuracy of the EAM has been shown through numerous applications to different metallic systems, including crystals, alloys, defects, surfaces, and interfaces, for which properties like stability, formation energies, phonon energies, etc. have been calculated.

The principle of this method is to split the total energy of the system into a sum over atomic components,

$$E_{\mathrm{tot}} = \sum_i E_i. \tag{1}$$

E_i is split into two parts. Of these, the embedding energy F for the ith atom is obtained by considering this atom as an impurity embedded into a host consisting of all the other atoms. The remaining part of the atomic energy is represented as short-ranged pair potentials. Accordingly,

$$E_i = F(\rho_i^h) + \tfrac{1}{2}\sum_{i \neq j} \phi(r_{ij}) \tag{2}$$

where ρ_i^h is the local electron density at site i and r_{ij} is the distance between atoms i and j.

The local electron density at site i is assumed being a superposition of atomic electron densities

$$\rho_i^h = \sum_{j(\neq i)} \rho_j^a(r_{ij}), \tag{3}$$

where $\rho_i^a(r_{ij})$ is the spherically averaged atomic electron density provided by atom j.

The EAM versions of Daw, Baskes, and Foiles (DBF) and of Voter and Chen (VC) differ first of all in the form of the pair potentials and in the set of systems for which the parameters entering the pair potentials have been parametrized. In the DBF version mainly properties of the infinite crystals were included in the fitting, whereas also properties of small systems like the dimer were included in the VC version.

In our earlier studies[56,57] we have calculated the geometries of the four lowest-energy structures of Ni_N clusters with N up to 150 using the DBF potential. These studies showed a very good agreement with experimental and other theoretical studies. Accordingly, it suggests that the bulk embedding functions and potentials for nickel are applicable also to smaller clusters with many low-coordinated atoms. This very important result was at the same time somewhat unexpected. In a smaller recent study[58] we compared directly the geometries and the energetics of the ground-state structures of nickel, copper, and gold clusters with N up to 160 atoms, obtained with the DBF and VC versions of the EAM. The results for Cu_N and Ni_N clusters suggested that the two potentials for these materials provide very similar results, which was lesser the case for gold. However, only little further information on the properties of the clusters was given. Thus, our reason for choosing the EAM was dictated by the generality of the EAM functionals, by the good agreement with experiment, as well as with results of first principles calculations, and by the high computational efficiency allowing one to investigate clusters with more than 100 atoms without severe constraints on the initial geometry, which is impossible with first principles methods.

In addition to the EAM we also used the many-body Gupta potential described in Ref. 49 as well as the Sutton-Chen potential. For the latter we did not optimize the structures but used the results from the Cambridge Cluster Database.[59] Copper is to be described by the so-called 9-6 potential and by scaling appropriately the results from the database we immediately obtain both structural and energetic properties.

TABLE I. The calculated bond length (in Å) and binding energy per atom (in eV/atom) of the copper dimer in comparison with the experimental and other semiempirical values. DBF and VC are the embedded-atom results of the present study, whereas *n*G and SC represent the results for the many-body Gupta potential and the Sutton-Chen potential, respectively. The last entry shows experimental results.

Cu_2	R(Å)	E_{bin}
DBF	2.15	1.22
VC	2.23	1.04
*n*G	2.23	1.29
SC	2.09	1.67
Expt.	2.22	1.02

B. Structure optimization

Using expression (1) we can calculate the total energy of any cluster with any structure as a function of the atomic coordinates $\{\mathbf{R}_i\}$, $E_{\text{tot}}(\mathbf{R}_1, \mathbf{R}_2, \ldots, \mathbf{R}_N)$. In order to obtain the closest local total-energy minimum we use the *variable metric/quasi-Newton* method.[60] We found that this was significantly more efficient than, e.g., the *conjugate gradient* method.

For searching the global minima we have developed our own *Aufbau/Abbau* method. It has been described in detail elsewhere[56] and shall, therefore, not be discussed in any detail here. We shall only emphasize that our method combines randomness with regularity and is significantly more efficient compared to the case when only random starting geometries are used. In addition, it is completely unbiased. However, it shall also be mentioned that no method can guarantee that the structure of the global total-energy minimum will be found. In our method it turned out to be very difficult to obtain a decahedral structure for $N=75$ that, therefore, was added to our pool of geometries. Moreover, through careful bookkeeping the method allowed us to identify the three energetically lowest-lying isomers of any Cu_N cluster.

We used this approach for the DBF version of the EAM for $2 \leqslant N \leqslant 150$, for the VC version for $2 \leqslant N \leqslant 60$, and for the many-body Gupta potential also for $2 \leqslant N \leqslant 60$. As mentioned above, for the Sutton-Chen potential we used scaled results from the Cambridge Cluster Database.[59]

III. RESULTS AND DISCUSSION

A. Accessing the accuracy of the approaches

As discussed in the introduction, the smallest copper clusters have been the topic of a number of studies using a variety of different approaches. The computational efforts to calculate the total energy for a given structure are relatively limited and, moreover, the number of metastable structures is small, too, thus, in total, making possible detailed and accurate studies of the properties of these smaller systems. Therefore, they are excellent systems for studying the accuracy of our approach.

The simplest possible system is, except for the trivial case of a single atom, the dimer, Cu_2. In Table I we show the calculated bond length and binding energy for this system as obtained with different theoretical methods in comparison with the experiment.[61] That the DBF version of the EAM does not perform so well as the VC version should not surprise, as the latter has been parametrized explicitly to the dimer properties, but otherwise most methods give fairly accurate results, with the Sutton-Chen potential being an exception.

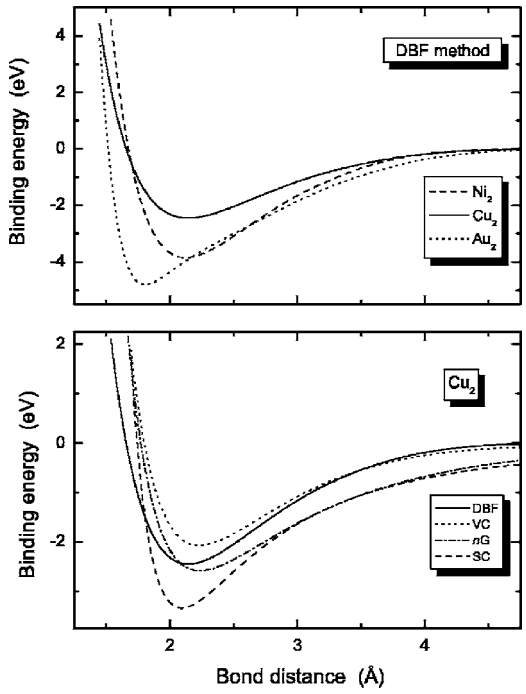

FIG. 1. The upper part shows the binding energy of the Cu, Ni, and Au dimers calculated with the DBF approach, whereas the lower part shows the binding energy of the Cu dimer as calculated with different theoretical methods. The methods are labeled according to Table I.

In order to get more detailed information about the differences between the various approximate methods, we calculated the binding energy as a function of the bond length for the copper dimer using different methods, as well as the same quantity for Ni_2 and Au_2. The results are shown in Fig. 1. One sees that the potential curves for Cu and Ni are almost identical in shape although differently scaled. The curve for the gold dimer has a completely different shape and, in addition, a deeper minimum. The short interatomic distances are crucial for the dimers, but for the larger clusters also the first- and second-neighbor interatomic distances play an important role. The potential curves for Ni_2 and Cu_2 approach each other rapidly, whereas the gold curve is always shifted, which makes us suggest that copper and nickel clusters are similar, but different from gold clusters. We shall return to the possible similarity between copper and nickel clusters below.

When comparing the different potentials for copper, i.e., the lower panel of Fig. 1, we see that the two EAM curves are very similar, in particular for larger interatomic distances, while the Gupta and the Sutton-Chen potentials show a different behavior. This suggests that the two EAM potentials

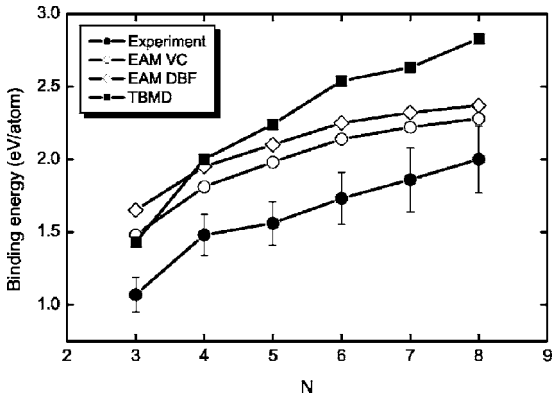

FIG. 2. The binding energy as a function of the cluster size as obtained with different theoretical methods in comparison with the experiment. EAM, VC, DBF, and TBMD denote the embedded-atom method (EAM) in the parametrization of Voter and Chen (VC) or of Dow, Baskes, and Foiles (DBF) as well as tight-binding molecular-dynamics (TBMD) results. The latter are from Ref. 28.

will give very similar results for larger clusters.

The smallest clusters with N up to around 10 have also a small number of (meta-)stable structures, which means that the global-minima structures can be fairly easy identified, so that a comparison between different methods can be made. In Fig. 2 we compare the binding energy as a function of cluster size as obtained with different theoretical methods in comparison with experiment.[62] Here, we have also compared with results of tight-binding molecular-dynamics calculations from Ref. 46. The close similarity of the two EAM methods with each other and with experimental results (except for a constant shift) is clearly recognized and provides confidence in the EAM for the copper clusters, at least concerning the total energy.

Also the structural properties of Cu clusters are well reproduced with the EAM. This can, e.g., be extracted from Table II, where we compare the symmetries of up to the three energetically lowest isomers for clusters with up to 10 atoms. From the results in the table we learn that only for Cu_7 all methods agree upon the symmetry of the energetically lowest structure. Moreover, for the absolutely smallest clusters with 3 and 4 atoms, there seems to be a tendency for the approximate methods (the embedded-atom method, the Sutton-Chen potential, and the many-body Gupta potential) to predict more compact structures than found by the other methods. For the larger systems there may be some differences regarding the energetic ordering of the isomers, but in total no method appears immediately as being significantly less accurate in predicting the symmetry of the small clusters.

In passing we add that the Cu_7 cluster is the first one containing the C_5 symmetry axis, an important element of the icosahedral and decahedral symmetries.

In total, we have seen that using the EAM method one obtains results that are accurate also for the smallest possible system. Compared to the Sutton-Chen and many-body Gupta potentials, the EAM potentials appear to be of shorter range. This may give rise to some structural differences for larger clusters when comparing the different approaches: For the EAM methods the longer-range interactions are weaker than with some of the other methods. We shall return to this issue below. But having established the accuracy of the EAM methods we shall now first of all present results from our EAM calculations on Cu_N clusters with N up to 150 using the DBF potential.

B. Energetic properties

The high stability of the so-called "magic-numbered" clusters has become a subject of great interest. In order to identify those particularly stable clusters, we have used the following criterion. A cluster is considered particularly stable if its binding energy per atom is larger than that of the two neighboring clusters. This can be quantified through the stability function,

$$\Delta_2(N) = E_{\mathrm{tot}}(N+1.1) + E_{\mathrm{tot}}(N-1.1) - 2E_{\mathrm{tot}}(N.1), \quad (4)$$

where $E_{\mathrm{tot}}(N.k)$ is the total energy of the energetically k-lowest isomer of the Cu_N cluster. This function, that has maxima for particularly stable clusters, is shown in Fig. 3. Here we can identify a large number of particularly stable clusters. These are found for $N=13$, 19, 23, 28, 46, 49, 55, 71, 75, 86, 92, 95, 101, 116, 119, 131, and 147. The most pronounced peaks occur at $N=13$, 55, and 147, corresponding to the formation of the first, the second, and the third Mackay icosahedra. Recent experimental studies[11] suggest that the Cu_{55} icosahedron is the global total-energy minimum for this cluster size. For Cu_{38} and Cu_{75}, a cuboctahedron and a Marks decahedron were obtained, in agreement with previous studies.[32,33] Only the work of Kabir *et al.*[46] predicts a structure with icosahedral symmetry as the global minimum of Cu_{38}, which was obtained by us as the energetically second-lowest isomer.

When comparing to our earlier results for Ni clusters,[56] we find many common trends in accordance with the observation above that the interatomic potentials for these two metals are similar. Nevertheless, there are also many differences. Thus, in the range $75<N<116$ the growth pattern is very different between Ni and Cu clusters, with the above-mentioned $N=86$, 92, and 95 being magic numbers for Cu, whereas Ni does not have particularly stable cluster sizes in this range. Second, the structures of the most stable Cu_N clusters for $92\leqslant N\leqslant 95$ are tetragonal, whereas no such structures are found for the same values of N for Ni_N. Third, as we found for the Ni clusters, also for Cu clusters in the size range $72\leqslant N\leqslant 82$ there is a competition between more different structures, i.e., icosahedral, decahedral and fcc-derived structures, with, however, material-specific differences. In Fig. 4 we illustrate this aspect. Here, we see that in particular for $N=79$ more structural motifs compete with the global total-energy minimum being found for a truncated centered octahedron and the two energetically higher isomers all corresponding to decahedra. Further we could detect that even the smallest copper clusters sometimes differ significantly from the corresponding nickel ones. For example, up to $N=12$ the global minima and the two higher-lying isomers of the two metals have the same symmetries, but already the second isomer of Cu_{13} has a higher symmetry (D_{5h}) than the "disordered" (C_s) second isomer of Ni_{13}. The third isomer of

TABLE II. The point groups for the smallest Cu_N clusters from different theoretical studies. DBF and VC denote the two different embedded-atom potentials, whereas *n*G, AI, TBMD, LMTO, and SC mark many-body Gupta, *ab initio*, tight-binding molecular dynamics, full-potential muffin-tin orbital based molecular dynamics, and the Sutton-Chen potential, respectively. Moreover, the Sym(k) is the point group for the isomer number k.

N	Ref.	Method	Sym(1)	Sym(2)	Sym(3)	N	Ref.	Method	Sym(1)	Sym(2)	Sym(3)
3	Here	DBF	D_{3h}			7	Here	DBF	D_{5h}	C_{3v}	C_2
	Here	VC	D_{3h}				Here	VC	D_{5h}	C_{3v}	C_2
	Here	*n*G	D_{3h}				Here	*n*G	D_{5h}	C_{3v}	C_2
	25	AI	C_{2v} (ob.)	C_{2v} (ac.)			27	AI	D_{5h}	C_{3v}	C_{2v}
	26	AI	C_{2v} (ob.)	C_{2v} (ac.)	D_{3h}		28	LMTO	D_{5h}	C_{3v}	C_{3v}
	27	AI	$D_{\infty h}$	D_{3h}			39	TBMD	D_{5h}	C_{3v}	C_{3v}
	28	LMTO	C_{2v} (ob.)				32	SC	D_{5h}		
	39	TBMD	C_{2v} (ob.)	D_{3h}	$D_{\infty h}$	8	Here	DBF	D_{2d}	C_s	D_{3d}
	32	SC	D_{3h}				Here	VC	D_{2d}	C_s	D_{3d}
4	Here	DBF	T_d				Here	*n*G	D_{2d}	C_s	D_{3d}
	Here	VC	T_d				27	AI	D_{4d}	C_{2v}	T_d
	Here	*n*G	T_d				28	LMTO	C_s	D_{2d}	
	26	AI	D_{2h}	D_{4h}	T_d		39	TBMD	C_s	O_h	D_{2d}
	27	AI	D_{2h}	C_{2v}	D_{4h}		32	SC	D_{2d}		
	28	LMTO	D_{2h}	D_{4h}	T_d	9	Here	DBF	C_{2v}	D_{3h}	C_{2v}
	39	TBMD	D_{2h}	D_{4h}	T_d		Here	VC	C_{2v}	D_{3h}	C_s
	32	SC	T_d				Here	*n*G	C_{2v}	D_{3h}	C_1
5	Here	DBF	D_{3h}				27	AI	C_s	C_s	C_s
	Here	VC	D_{3h}				28	LMTO	D_{3h}	C_{2v}	
	Here	*n*G	D_{3h}				39	TBMD	C_2	C_{2v}	C_s
	26	AI	C_{2v}	D_{3h}	C_{4v}		32	SC	C_{2v}		
	27	AI	C_{2v}	D_{3h}	C_{4v}	10	Here	DBF	C_{3v}	D_{2h}	C_2
	28	LMTO	D_{3h}	C_{4v}			Here	VC	C_{3v}	D_{4d}	C_2
	39	TBMD	C_{2v}	D_{3h}			Here	*n*G	C_{3v}	C_2	C_{2v}
	32	SC	D_{3h}				27	AI	C_s		
6	Here	DBF	O_h	C_{2v}			32	SC	C_{3v}		
	Here	VC	O_h	C_{2v}							
	Here	*n*G	O_h	C_{2v}							
	25	AI	D_{3h}	C_{5v}	C_{2v}						
	27	AI	C_{5v}	D_{3h}	C_s						
	28	LMTO	C_s	O_h							
	39	TBMD	C_{5v}	C_{2v}	O_h						
	32	SC	O_h								

Cu_{13} is an octahedron, a statement which we have not seen published before. The ground states of Cu_{15}–Cu_{17} differ significantly from the nickel ones in favor of the higher-symmetrical structures, however, the double icosahedron at $N=19$ is common for both metals. The highly symmetrical structure at $N=22$—a capped hexagonal double antiprism—is the global minimum only of the corresponding copper cluster.

It is interesting to compare the present results with those of Kabir *et al.*[46] The authors used a parametrized tight-binding model (i.e., a model that explicitly includes the electronic orbitals in contrast to our approach) together with a molecular dynamics technique for the relaxation of selected initial configurations of Cu_N clusters with N up to 55, in order to search for the global energy minima. The fact that a single Cu atom has an odd number of electrons was clearly recognized in an even-odd oscillation in the stability function, so that essentially only clusters with an even N were found to be particularly stable. Moreover, the stability function was found to span an overall larger energy range, i.e., from −3 to +3 eV. It is not clear whether the more limited geometry optimization in the study of Kabir *et al.*[46] or the explicit inclusion of the electronic orbitals is responsible for the difference with our results.

Another possible criterion for the occurrence of a particularly stable cluster is to require that the energy difference between the two energetically lowest isomers $E_{tot}(N.2) - E_{tot}(N.1)$ is large. This energy difference together with the

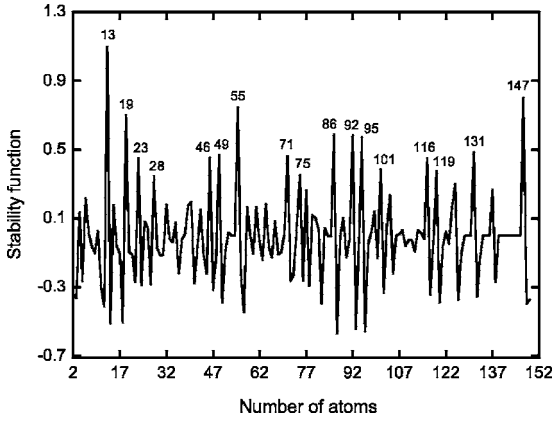

FIG. 3. The stability function as a function of cluster size.

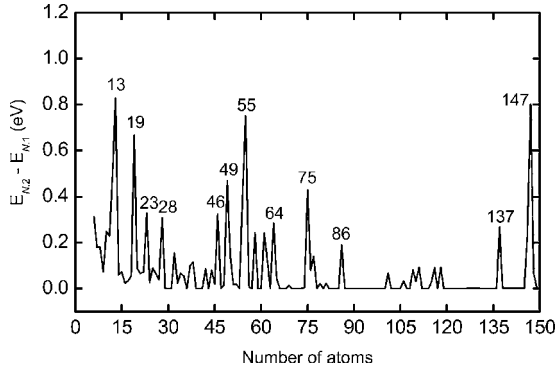

FIG. 5. The total-energy difference between the two energetically lowest isomers as a function of the cluster size.

energy differences to the energetically higher ones are shown in Fig. 5. For $N \leqslant 55$ it is striking that the energetically higher-lying isomers become energetically less and less separated and, as seen when comparing with Fig. 3, many of the clusters that are particularly stable according to the first criterion are also according to the second one. For $N > 55$ only the peaks at $N=64$, 75, 86, 137, and 147 are common for both figures.

Figure 5 shows that for the smallest clusters, that were discussed in the previous subsection, the total-energy differences between the energetically lowest isomers are no more than roughly 0.2 eV per cluster (i.e., much less than room temperature for $N=20$). This can explain why different theoretical methods give different energetic orderings of the isomers, cf. Table II: For the clusters with some 5–10 atoms, there may be of the order of 20 interatomic interactions, indicating that these have to be given with an accuracy of 10 meV in order to obtain the correct isomer ordering.

In Fig. 6 we compare the binding energies per atom for the different potentials for N up to 60. The stronger nearest-neighbor interaction of the DBF potential compared to the VC potential, cf. Fig. 1, can explain the difference between the binding energies obtained with those two. On the other hand, the SC and nG potentials are in general (cf. Fig. 1) more bonding than the EAM potentials, but nevertheless the binding energy per atom is not generally larger for those

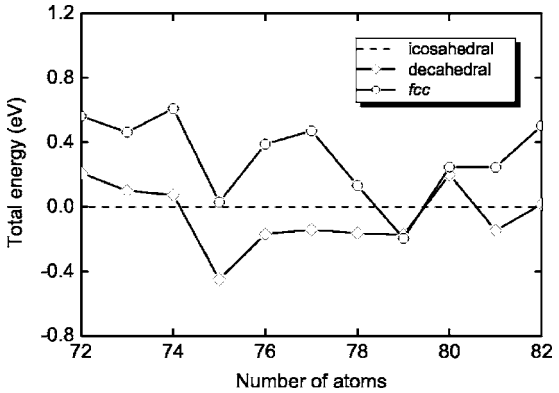

FIG. 4. The relative total energy of the icosahedral, decahedral, and fcc-derived clusters as a function of the cluster size for $72 \leqslant N \leqslant 82$.

potentials. However, as we shall see below, these potentials yield structures that are somewhat different from those of the EAM potentials. Then, the difference in the binding energy results from a subtle interplay of nearest-neighbor-interaction differences and structural differences.

C. Structural properties

We have used the DBF potential in optimizing the structures for the three energetically lowest isomers for Cu_N for N up to 150, whereas the same approach was used for the VC and nG potentials for N up to 60. Finally, for the SC potential we have used scaled results from the Cambridge Cluster Database[59] also for N up to 60, giving the single energetically lowest isomer. Instead of discussing the structures of the individual clusters, we shall here focus on drawing more general conclusions about the properties of these small particles.

First we shall consider the overall shape of the clusters. As we showed in our earlier report on Ni clusters,[56] it is convenient to study the 3×3 matrix containing the elements $I_{st} = (1/u_l^2) \Sigma_{n=1}^{N} (R_{n,s} - R_{0,s})(R_{n,t} - R_{0,t})$ with $u_l = 1$ Å being a length unit, and s and t being x, y, and z, and with $\mathbf{R}_0 = (1/N) \Sigma_{n=1}^{N} \mathbf{R}_n$ being the center of the cluster. The three eigenvalues of this matrix, $I_{\alpha\alpha}$, can be used in separating the clusters into being overall spherical (all eigenvalues are identical), more cigar-like shaped (one eigenvalue is large, the other two are small), or more lens-shaped (two large and one small eigenvalue). The average of the three eigenvalues, $\langle I_{\alpha\alpha} \rangle$, is a measure of the overall extension of the cluster. For a homogeneous sphere with N atoms, the eigenvalues scale like $N^{5/3}$. Hence, we show in Fig. 7 quantities related to $I_{\alpha\alpha}$ but scaled by $N^{-5/3}$.

One can see that only few clusters have an overall spherical shape (these are found for the energetically lowest isomer for $N=4$, 6, 13, 17, 26, 28, 38, 55, 79, 92, and 147, for the second one $N=54$ and 146, and for the third one $N=13$, that all correspond to high-symmetric isomers (cf. Table II) and, for the lowest-energy isomer most of them to the class of magic clusters. There are some larger intervals in which all the three isomers possess similar shapes, i.e., for $15 < N < 24$, $30 < N < 38$, $56 < N < 65$, $68 < N < 74$, and $95 < N < 101$, where all isomers have cigar-like shape, and for 38

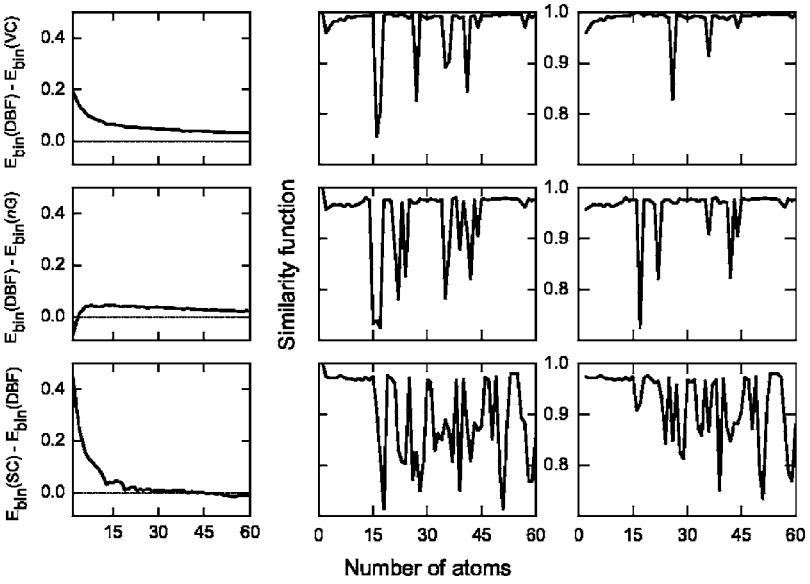

FIG. 6. The left column shows the differences in the binding energies in eV/atom between the DBF clusters and those optimized with (from top to bottom) the VC potential, the many-body Gupta, and the Sutton-Chen 9-6 potential. The middle column shows the similarity function for the comparison between the structures of the energetically lowest isomers obtained with the same pair of potentials. The right column shows the same results as in the middle column except for a comparison between the energetically lowest DBF isomer and the structurally most similar isomer obtained with the other methods. An exception is the lowest panel where due to the lack of information the energetically lowest isomer of the SC clusters was compared to all the three isomers of the DBF clusters.

$<N<53$, $80<N<90$, and $111<N<136$ where the lens shape dominates. With few exceptions ($Cu_{23.3}$, $Cu_{25.2}$, $Cu_{28.2}$, and $Cu_{81.1}$) the average value is very similar for all three isomers. The lower panel in Fig. 7 shows that there are size ranges, e.g., around $N=55$ and $N=92$ and for $N\geqslant 140$, where the three eigenvalues are very close, although not necessarily identical, so that for these clusters the overall shape is close to spherical. Figure 7 indicates also that all three isomers for a given N have very similar shape.

Table III gives the symmetries of the optimized structures; for $N\leqslant 60$ for more different potentials. In most cases the different potentials give the same or very similar symmetries—at most with some reordering—lending support for our conclusions. Moreover, in those cases where deviations are found they occur almost exclusively for the lowest symmetries like C_s and C_1 where maybe only smaller structural changes are required in order to give a higher symmetry.

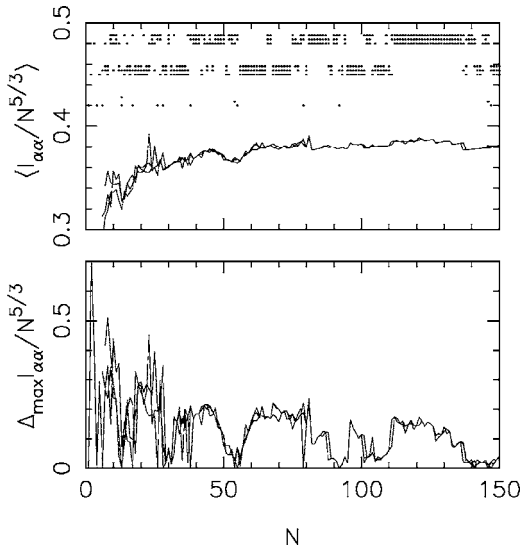

FIG. 7. Different properties related to the eigenvalues $I_{\alpha\alpha}$. In the upper panel we show the average value together with points indicating whether clusters with overall spherical shape (lowest set of rows), overall cigar shape (middle set of rows), or overall lens shape (upper set of rows) are found for a certain size. Moreover, in each set of rows, the lowest row corresponds to the energetically lowest isomer, the second one to the energetically second-lowest isomer, etc. In the lower panel we show the maximum difference of the eigenvalues for the three different isomers.

We have found earlier[56] that it was useful to monitor the structural development of the isomer with the lowest total energy through the so-called similarity functions. We define the radial distances from the center for each of the atoms of a given cluster Cu_N $r_n=|\mathbf{R}_n-\mathbf{R}_0|$ and sort these in increasing order.

Simultaneously we consider a large spherical fragment of a fcc crystal as well as a large cluster of icosahedral symmetry, here Cu_{309}. Also for these we define a radial distance for each atom, r'_n, which also are sorted. In order to compare a given cluster with those two systems we calculate subsequently $q=[(1/N)\Sigma_{n=1}^{N}(r_n-r'_n)^2]^{1/2}$, giving the similarity function $S=[1/(1+q/u_l)]$ ($u_l=1$ Å). S approaches 1 if the Cu_N cluster is very similar to the reference system, i.e., a fragment of the fcc crystal or an icosahedral cluster. In Fig. 8 we show the resulting functions in four cases, i.e., when comparing with the relaxed Cu_{309} cluster, and when comparing with three fragments of the fcc crystal differing in the position of the center (i.e., the position of an atom, the middle of a nearest-neighbor bond, and the center of the unit cell, respectively).

One sees both that clusters that clearly resemble fcc fragments and that clusters that resemble icosahedral clusters can be identified. The most pronounced peaks for the icosahedral structures correspond to $N=13$, 55, and 147, the first-, second-, and third-layer Mackay icosahedron, respectively. Clusters with icosahedral structures are also found in the interval between $N=75$ and $N=79$, as discussed in the previous subsection, where it also was mentioned (cf. Fig. 4) that in this size range the structures compete with fcc-derived ones. The octahedral ones are found around $N=6$, 8, 13, 28, 38, and 79. Beyond $N=135$, the values for the fcc-like clusters decrease, whereas an increased similarity with the icosa-

TABLE III. The point groups for the first three isomers for $N=11-150$ obtained in our study. For $11 \leqslant N \leqslant 60$ we give from above the results for the DBF, the VC, the many-body Gupta, and the SC potential, respectively. For the latter, only the first isomer has been considered. For $61 \leqslant N \leqslant 150$ we give only results for the DBF potential.

N	N.1	N.2	N.3	N	N.1	N.2	N.3	N	N.1	N.2	N.3	N	N.1	N.2	N.3	N	N.1	N.2	N.3	N	N.1	N.2	N.3	N	N.1	N.2	N.3
11	C_{2v}	C_2	C_{2v}	22	D_{6h}	C_1	C_s	33	C_2	C_s	C_s	44	C_s	C_1	C_1	55	I_h	C_s	C_s	81	C_{2v}	C_2	C_2	125	C_s	C_s	C_s
	C_{2v}	C_2	C_{2v}		D_{6h}	C_s	C_1		C_2	C_s	C_s		C_s	C_s	C_1		I_h	C_1	C_s	82	C_1	C_1	C_1	126	C_1	C_1	C_1
	C_{2v}	C_{2v}	C_2		C_s	C_s	C_s		C_2	C_s	C_s		C_1	C_s	C_1		I_h	I_h	C_s	83	C_3	C_3	C_3	127	C_{2v}	C_1	C_1
	C_{2v}				C_s				C_s				C_2				I_h			84	C_1	C_1	C_1	128	C_1	C_s	C_1
12	C_{5v}	C_1	D_{3h}	23	D_{3h}	D_2	D_{3h}	34	C_s	C_1	C_s	45	C_s	C_s	C_1	56	C_s	C_{3v}	C_{3v}	85	C_1	C_1	C_1	129	C_s	C_s	C_s
	C_{5v}	C_1	D_{3h}		D_{3h}	D_2	C_1		C_s	C_s	C_1		C_s	C_s	C_1		C_s	C_{3v}	C_{3v}	86	C_3	C_1	C_1	130	C_1	C_s	C_s
	C_{5v}	D_{3h}	C_1		D_{3h}	C_2	C_s		C_s	C_1	C_s		C_s	C_s	C_s		C_s	C_s	C_{3v}	87	C_1	C_1	C_1	131	C_{2v}	C_{2v}	C_1
	C_{5v}				C_2				C_2				C_s				C_s			88	C_1	C_1	C_s	132	C_1	C_1	C_1
13	I_h	D_{5h}	O_h	24	D_3	C_{2v}	C_s	35	C_{2v}	D_3	D_3	46	C_{2v}	C_1	C_s	57	C_1	C_1	C_s	89	C_{3v}	C_{3v}	C_{3v}	133	C_s	C_s	C_s
	I_h	C_s	C_s		D_3	C_{2v}	C_s		D_3	C_{2v}	C_{2v}		C_{2v}	C_1	C_s		C_s	C_1	C_s	90	C_s	C_s	C_s	134	C_{3v}	C_{3v}	C_{3v}
	I_h	C_s	C_s		C_{2v}	C_s	D_3		D_3	D_3	C_{2v}		C_{2v}	C_{2v}	C_1		C_s	C_s	C_s	91	C_1	C_1	C_1	135	C_s	C_s	C_1
	I_h				C_2				D_3				C_{2v}				C_s			92	T	T	T	136	C_s	C_s	C_s
14	C_{3v}	C_{2v}	C_s	25	C_3	C_{2v}	C_1	36	C_s	C_1	C_1	47	C_1	C_1	C_1	58	C_{3v}	C_1	C_1	93	C_3	C_3	C_3	137	C_{3v}	C_{2v}	C_1
	C_{3v}	C_{2v}	C_{6v}		C_3	C_{2v}	C_1		C_1	C_1	C_2		C_1	C_1	C_s		C_{3v}	C_1	C_1	94	C_1	C_1	C_1	138	C_{3v}	C_s	C_s
	C_{3v}	C_{2v}	C_1		C_3	C_{2v}	C_s		C_s	C_1	C_2		C_1	C_s	C_1		C_{3v}	C_1	C_s	95	C_1	C_1	C_1	139	C_{2v}	C_s	C_s
	C_{3v}				C_3				C_{2v}				C_1				D_{3h}			96	C_{2v}	C_{2v}	C_{2v}	140	C_s	C_s	C_{5v}
15	D_{6d}	C_{2v}	C_{2v}	26	T_d	C_1	C_{2v}	37	C_2	C_1	C_3	48	C_s	C_s	C_s	59	C_1	C_1	C_{3v}	97	C_{2v}	C_{2v}	C_{2v}	141	C_{5v}	C_{3v}	C_2
	D_{6d}	C_{2v}	C_{2v}		T_d	C_1	C_{2v}		C_2	C_3	C_1		C_s	C_s	C_s		C_1	C_s	C_{2v}	98	C_s	C_s	C_s	142	C_s	C_s	C_{5v}
	C_{2v}	D_{6d}	C_{2v}		T_d	C_1	C_s		C_2	C_3	C_{3v}		C_s	C_s	C_s		C_1	C_{2v}	C_{3v}	99	C_{2v}	C_{2v}	C_{2v}	143	C_{2v}	C_s	C_s
	D_{6d}				D_{3h}				C_{3v}				C_{2v}				T_d			100	C_s	C_s	C_s	144	C_{3v}	C_s	C_s
16	D_{3h}	C_s	C_s	27	C_{2v}	C_s	C_s	38	O_h	C_5	C_5	49	C_{3v}	C_1	C_1	60	C_s	C_s	C_s	101	D_{5h}	D_3	C_s	145	C_{2v}	C_{2v}	C_s
	C_s	C_s	D_{3h}		C_s	C_{2v}	C_s		O_h	C_{5v}	D_{4h}		C_{3v}	C_1	C_s		C_s	C_1	C_1	102	C_{2v}	C_{2v}	C_{2v}	146	C_{5v}	I_h	C_s
	C_s	C_s	D_{3h}		C_{2v}	C_s	C_s		O_h	I_h	C_{5v}		C_{3v}	C_s	C_1		C_s	C_1	C_s	103	C_s	C_s	C_{2v}	147	I_h	C_1	C_1
	C_s				C_s				O_h				C_{3v}				C_{2v}			104	C_2	C_1	C_{2v}	148	C_s	C_s	C_s
17	T_d	C_2	C_2	28	T	D_2	C_1	39	C_5	C_5	C_5	50	C_s	C_1	C_1	61	C_{2v}	C_s	C_s	105	C_2	C_s	C_s	149	C_s	C_s	C_s
	C_2	T_d	C_2		T	C_2	D_2		C_5	C_{4v}	C_s		C_s	C_s	C_s	62	C_1	C_{2v}	C_s	106	C_1	C_s	C_1	150	C_{3v}	C_{3v}	C_{3v}
	C_2	C_s	C_s		T	C_1	C_s		C_{5v}	C_5	C_{4v}		C_s	C_s	C_s	63	C_1	C_1	C_1	107	C_{2v}	C_{2v}	C_s				
	C_{2v}				C_1				C_{4v}				D_{3h}			64	C_s	C_1	C_1	108	C_s	C_s	C_s				
18	C_s	C_{5v}	C_{2v}	29	C_3	C_3	C_3	40	C_s	C_s	C_s	51	C_{2v}	C_s	C_s	65	C_1	C_1	C_1	109	C_1	C_{2v}	C_1				
	C_s	C_{5v}	C_2		C_3	C_{2v}	C_2		C_s	C_2	C_s		C_{2v}	C_s	C_s	66	C_1	C_1	C_1	110	C_s	C_s	C_s				
	C_s	C_{5v}	C_s		C_3	C_{2v}	C_2		C_s	C_s	C_s		C_{2v}	C_s	C_s	67	C_2	C_2	C_2	111	C_{2v}	C_1	C_1				
	C_{2v}				C_2				C_s				C_s			68	C_1	C_1	C_1	112	C_s	C_s	C_s				
19	D_{5h}	C_1	C_1	30	C_s	C_s	C_1	41	C_1	C_1	C_1	52	C_{3v}	C_s	C_s	69	C_1	C_1	C_1	113	C_s	C_s	C_s				
	D_{5h}	C_1	C_1		C_s	C_1	C_s		C_3	C_1	C_s		C_{3v}	C_s	C_s	70	C_1	C_1	C_5	114	C_s	C_s	C_s				
	D_{5h}	C_s	C_1		C_s	C_1	C_1		C_s	C_s	C_1		C_{3v}	C_s	C_s	71	C_5	C_1	C_5	115	C_{5v}	C_s	C_{5v}				
	D_{5h}				C_s				C_s				C_{2v}			72	C_s	C_s	C_s	116	C_{5v}	C_5	C_5				
20	C_{2v}	D_{3d}	D_2	31	C_3	C_3	C_3	42	D_2	C_{2v}	C_2	53	C_{2v}	D_{5d}	C_{2v}	73	C_s	C_1	C_s	117	C_1	C_1	C_1				
	C_{2v}	D_2	D_{3d}		C_3	C_s	C_{2v}		D_2	C_s	C_s		C_{2v}	D_{5d}	C_{2v}	74	D_{3d}	C_{2v}	C_2	118	C_s	C_s	C_s				
	C_{2v}	D_2	D_{3d}		C_3	C_s	C_s		C_s	C_s	C_s		C_{2v}	D_{5d}	C_{2v}	75	D_{5h}	C_s	C_s	119	C_s	C_s	C_s				
	C_{2v}				C_3				C_s				C_{2v}			76	C_s	D_2	C_s	120	C_1	C_1	C_1				
21	C_s	C_1	C_{2v}	32	D_3	C_{2v}	D_{2d}	43	C_s	C_s	C_s	54	C_{5v}	I_h	C_{2v}	77	C_{2v}	C_1	C_1	121	C_1	C_1	C_1				
	C_s	C_1	C_2		D_3	D_{2d}	C_{2v}		C_s	C_1	C_2		C_{5v}	I_h	C_{2v}	78	C_1	C_1	C_1	122	C_1	C_1	C_1				
	C_1	C_{2v}	C_s		D_3	C_{2v}	C_{2v}		C_s	C_s	C_1		C_{5v}	C_{5v}	I_h	79	O_h	C_{2v}	C_{2v}	123	C_s	C_s	C_s				
	C_1				D_{2d}				C_s				C_{5v}			80	C_2	C_2	C_2	124	C_s	C_s	C_s				

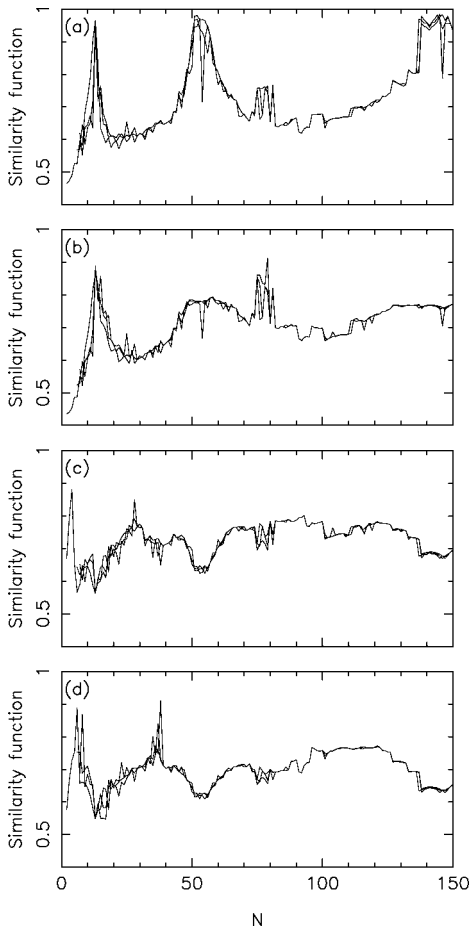

FIG. 8. Each panel shows the similarity function for all the three isomers when comparing to (a) an icosahedral cluster, and (b)–(d) a spherical fragment of the fcc crystal where the center of the fragment is placed at (b) the position of an atom, (c) the middle of a nearest-neighbor bond, and (d) the center of the unit cell, respectively.

hedral clusters is observed. It is interesting to notice that the structures are built up over a certain range of cluster sizes so that, e.g., the icosahedral structure for $N=55$ can be seen also for both larger and smaller values of N around this value.

We can also use the concept of similarity functions to compare the structures of Cu_N isomers for $N \leqslant 60$ as calculated using different potentials. This comparison is shown in Fig. 6, too. From the upper-most panels we learn that the two different EAM potentials most often give very similar structures, in particular if we allow for a reordering of the energetic order of the isomers, as shown in the right panel. This may not surprise when taking the similarity of the potentials into account, cf. Fig. 1. A similar agreement, although less pronounced, may also be recognized when comparing the many-body Gupta and the DBF EAM results in Fig. 6, whereas the SC potential seems to predict quite different structures.

The examination of the behavior of the four potentials shows that the EAM and the Gupta potentials yield structures which are structurally and energetically alike, while the overbinding in the Sutton-Chen potential leads to shorter

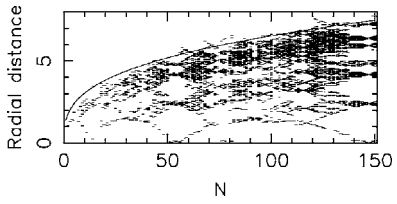

FIG. 9. The radial distribution (in Å) for the energetically lowest isomer. First (upper panel), each small line represents (at least) one atom with that radial distance. The smooth curve marks the radius of a sphere with the atomic density as in fcc Cu as a function of number of atoms.

bond lengths and, hence, large structural differences compared to the EAM and the Gupta potentials.

The distribution of the radial distances as function of the cluster size in all the clusters is shown in Fig. 9 for the energetically lowest isomer. For the next two isomers very similar results are obtained, showing that the structures of the lowest-lying isomers are closely related. For the sake of completeness, we add that the sometimes chaotic appearance in Fig. 9 is partly related to the presentation: For a cluster consisting of a high-symmetric core plus one extra atom on the surface, the radial distances will only partly reflect the existence of the highly symmetric core.

Returning to the figure, we see that up to N around 50 there are two small atomic-shell constructions, corresponding to the energetically lowest isomers of Cu_{13} and Cu_{38}, but for N just above 50 a clear tendency towards shell-construction can be seen. This corresponds to the formation of the Cu_{55} icosahedron. In the interval $N=70-140$, numerous smaller shell constructions can be observed, which in turn means, that the cluster growth is regular, and corresponds to the constructions of typical symmetrical shells, that the *icosahedral* and the fcc clusters possess. Also for N above 137 clear shell constructions for all the isomers are seen. This corresponds to the formation of the third Mackay icosahedron, Cu_{147}. To our knowledge, this is the first time that this icosahedron is obtained in *unbiased* calculations.

Further structural properties are presented in Fig. 10. The binding energy per atom, and the average bond lengths of the clusters are presented together with their *bulk* values. Also the trends in the coordination in the clusters are shown. Here, we have defined two atoms as being bonded if their interatomic distance is less than 3.09 Å, which is the average value between the nearest-neighbor distance (2.56 Å) and the next-nearest-neighbor distance (3.62 Å) in bulk Cu. Maybe not surprisingly, it is obvious from the figure that the *bulk* values have not at all been reached within the size range of this study. Our study on nickel clusters[56] showed that even at $N=2500$, the bulk value of the binding energy was not yet reached. Hence, one should optimize clusters containing probably 10 000 atoms or more in order to reach the bulk binding energy.

The minimal atomic coordination for each cluster size is shown in Fig. 10(c). The existence of low-coordinated atoms, i.e., with coordination numbers of 3 or 4, may suggest

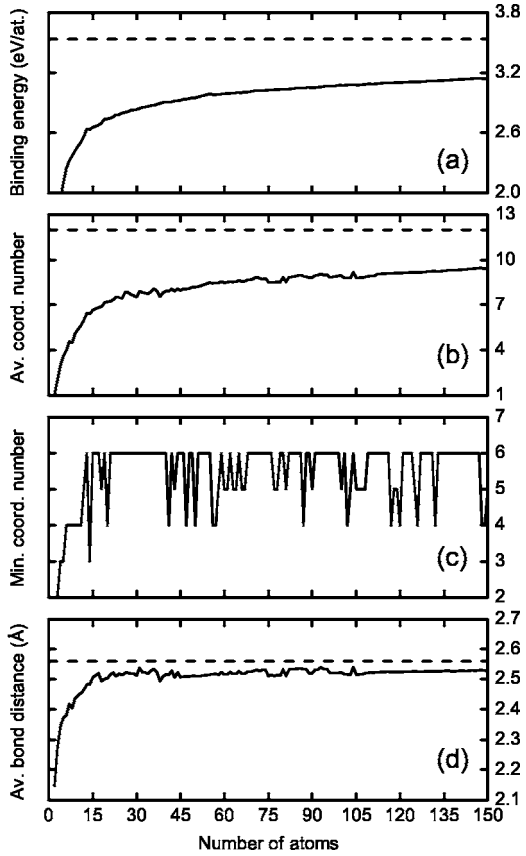

FIG. 10. (a) The binding energy per atom, (b) the average coordination number, (c) the minimum coordination number, and (d) the average bond distances as functions of the cluster size. The dashed lines in (a), (b), and (d) show the corresponding bulk values.

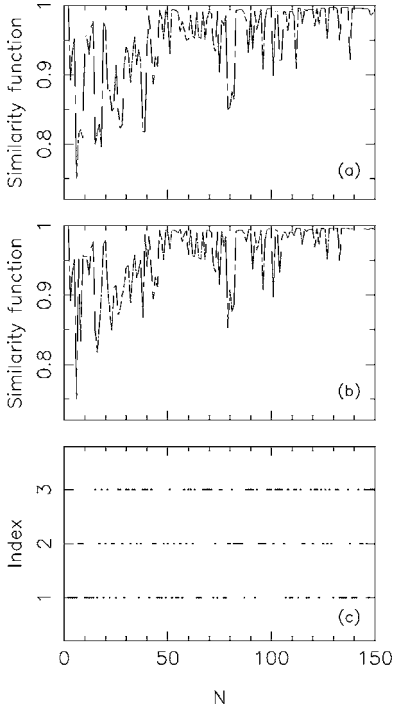

FIG. 11. (a) and (b) show the similarity functions that describe whether the cluster with N atoms is similar to that of $N-1$ atoms plus an extra atom, when (a) only considering the lowest-energy isomer for the $(N-1)$-atom cluster and (b) considering all the three isomers of that cluster. (c) Shows which isomer in the latter case is most similar to the one with N atoms.

the occurrence of a cluster growth where extra atoms are added to the surface of the cluster, whereas the larger minimal coordination numbers could indicate a growth where atoms are inserted inside the cluster, or, alternatively, upon a strong rearrangement of the surface atoms. This is the case for the clusters corresponding to $N=21-40$, $N=68-76$, 82–86, 91–99, 109–116, 121–124, 127–131, and $N=133-146$, where windows with high coordination number are found. The low-coordinated clusters have $N=14$, 20, 41, 47, 50, 56, 57, 87, 102, 117, 120, 126, 132, and 148. Most of them correspond to highly symmetrical structures with one additional atom, for example those with $N=14$, 56, and 148. Figure 10(d) shows the average bond length as function of cluster size. Since many of the atoms for the clusters of the present study are at or close to the surface, their coordination is lower than in the bulk and, accordingly, they tend to form bonds of shorter length than in the bulk. Therefore, it may not surprise that the average bond length is smaller than that of the bulk, and that this effect is most pronounced for the smallest clusters. This finding is also recognized in Fig. 9, where it is seen that the largest radial distance most often is well below the radius of a spherical part of crystalline Cu with the same number of atoms.

D. Growth patterns

In this subsection we shall attempt to identify how clusters grow and, in particular, if the cluster with N atoms can be derived from the one with $N-1$ atoms simply by adding one extra atom. In order to quantify this possible relation we consider first the structure with the lowest total energy for the $(N-1)$-atom cluster. For this we calculate and sort all interatomic distances, d_i, $i=1,2,\ldots,N(N-1)/2$. Subsequently we consider each of the N fragments of the N-cluster that can be obtained by removing one of the atoms and keeping the rest at their positions. For each of those we also calculate and sort all interatomic distances d_i', and calculate, subsequently, $q=[[2/N(N-1)]\Sigma_{i=1}^{N(N-1)/2}(d_i-d_i')^2]^{1/2}$. Among the N different values of q we choose the smallest one, $q_{\min}$ and calculate the similarity function $S=1/(1+q_{\min}/u_l)$ ($u_l=1$ Å) which approaches 1 if the Cu_N cluster is very similar to the Cu_{N-1} cluster plus an extra atom.

This function is shown in Fig. 11(a). We see that for N up to around 40, S is significantly different from 1, giving support to the consensus that in this range the growth is complicated and not simply an atom-to-atom addition to a given core. The most pronounced peaks occur at $N=6$, 9, 15–18, 27, 28, 38, 39, 42, 75, 79–82, 101, 112, and 138, for which, in most cases, the structures possess high symmetry. However, one may ask whether the second and the third isomers could play a role in the growth process, in particular when taking into account the fact that their total energies often differ only little. Accordingly, we examined whether the structure of the energetically lowest isomer of Cu_N would resemble *any* of the three energetically lowest isomers for

Cu_{N-1} in the same sense as above, i.e., we use the quantity q in quantifying the structural difference. From the three different values for q (for the three different isomers) we chose the smallest one and constructed the similarity function from that. The resulting function is presented in Fig. 11(b), and compared to Fig. 11(a) it is clearly seen that the complicated growth of the first isomers does not disappear when comparing to all the three isomers. This supports our previous conclusion (see Figs. 7–9) that for a given cluster size the three isomers resemble very much each other. One can see in Fig. 11(c) which of the three energetically lowest isomers of Cu_{N-1} leads to highest similarity with the Cu_N cluster, and from the fact that this only for the smaller N is most often the first isomer, we learn that the growth process is a complicated process where more different isomers are important, i.e., not only the energetically most stable ones, although these may resemble each other (cf. Fig. 9). This means that it is difficult to imagine that the growth occurs as a one-by-one addition of atoms to the energetically most stable isomers.

IV. SUMMARY AND CONCLUSIONS

Using an unbiased approach, we have determined the three energetically lowest isomers of copper clusters in the size range $2 \leqslant N \leqslant 150$ with the DBF version of the embedded-atom method. In the size range $2 \leqslant N \leqslant 60$ we also considered three other many-body potentials, i.e., the VC version of the embedded-atom method, the many-body Gupta potential, and the Sutton-Chen potential. To the best of our knowledge, the present study is the first one where the energetics and the structures of metal clusters derived with different model potentials are compared so comprehensively.

For the absolutely smallest clusters, $N \leqslant 6$, the model potentials all tended to produce more compact structures than what was found with parameter-free calculations, but beyond this size most potentials lead to very similar results regarding structure and energetics, with the Sutton-Chen. Also the Sutton-Chen results for Ni clusters were in conflict with both experimental and our theoretical (EAM) results (see Ref. 56 and references therein). Most likely the parametrization chosen in Ref. 32 for the many-body Sutton-Chen potential for Ni and Cu underestimates the stability of icosahedral packing and correspondingly overestimates stability of decahedral motifs. In many cases we found a change of the relative energetic order of the different isomers when comparing the different potentials, but taking into account that the energetic difference between the isomers is often only a few meV/atom this should not be surprising. Moreover, we found that all three isomers for a given N most often were structurally quite similar.

Our study predicts a number of particularly stable clusters, i.e., magic-numbered clusters, that in many cases are in agreement with the results obtained from first principles and other semiempirical studies when such exist, but the advantage of our study is that the structures were obtained by using a completely unbiased approach. These magic numbers were clearly visible both in the stability function and, in most cases, also in the total-energy difference between the energetically lowest and higher-lying isomers. To our knowledge, none of the previous studies concentrated on the higher-lying isomers. In the present work we have shown that the energy difference between the first and the next-lying isomer is as good a criterion for cluster stability, as is the stability function itself. Most of the highly stable clusters correspond to structures with high symmetry, such as $Cu_{13}(I_h)$, $Cu_{19}(D_{5h})$, $Cu_{55}(I_h)$, $Cu_{92}(T)$, and $Cu_{147}(I_h)$, but also highly stable clusters of low symmetry were found [e.g., $Cu_{46}(C_{2v})$, $Cu_{64}(C_s)$, and $Cu_{86}(C_3)$]. Moreover, this is the first time that the Cu_{147} icosahedron has been obtained in an unbiased structure optimization. Furthermore, our results for the size range $75 < N < 116$ demonstrate clearly the materials-specificity of many of the properties: In this range our optimized structures are markedly different from those we have obtained earlier for Ni_N clusters.[56]

In order to study the structural properties we analyzed the eigenvalues of the matrix containing the moments of inertia and introduced the so-called similarity functions. The latter indicated that all the three isomers we studied are very similar in most of the cases, and that roughly spherical clusters were found mainly for the energetically lowest isomer but in some cases also for the second-lowest one, and that these often correspond to particularly stable structures. A noteworthy example is Cu_{54} for which the second-lowest isomer has I_h symmetry, similar to the lowest isomer for Cu_{55} but without the central atom. The existence of this structure was suggested almost 10 years ago by Mottet *et al.*[63] but first in our study it was found.

By examining the similarity functions we could identify several clusters with fcc-like structures and three with icosahedral structure. Whereas the former occurred for N around 6, 13, 28, 38, and 79, the latter was found for N around 13, 55, and 147. It is interesting to notice that these structural motifs were built up over a larger range of N values and were, accordingly, not limited to those singular values of N. By analyzing the distribution of radial distances as a function of the cluster size we could identify several regions with N around 55, 75, and 147, where typical shell constructions occurred.

We also found that even for our largest clusters the binding energy per atom and the average bond distance have still not converged to the bulk limit. Similarly, the average coordination number is far from the bulk value, but higher than for nickel clusters, where several structures with shell constructions and corresponding low coordination numbers were formed.[56]

One of the most important general trends is that the cluster growth is generally multilayered icosahedral or layer by layer growth—from the one-shell Mackay icosahedron at $N=13$ to the two-shell icosahedron Cu_{55} and then to the 147-atom structure which is the third Mackay icosahedron. Cluster growth pattern between two closed-shell icosahedra is not simple. It is predominantly icosahedral with islands of fcc growth for Cu_6, Cu_{38}, and Cu_{79}, tetrahedral for Cu_4, Cu_{17}, Cu_{26}, $Cu_{28}-Cu_{29}$, and $Cu_{91}-Cu_{95}$, and decahedral for $Cu_{75}-Cu_{78}$, Cu_{81} and $Cu_{101}-Cu_{103}$. These islands are material-specific and differ from those deduced for nickel clusters.[56]

ACKNOWLEDGMENTS

We gratefully acknowledge *Fonds der Chemischen Industrie* for very generous support. This work was supported by the SFB 277 of the University of Saarland and by the German Research Council (DFG) through Project No. Sp439/14-1.

*Corresponding author. Email: vg.grigoryan@mx.uni-saarland.de
†Email: deni@springborg.pc.uni-sb.de
‡Email: m.springborg@mx.uni-saarland.de

[1] M. De Crescenzi, M. Diociaiuti, L. Lozzi, P. Picozzi, and S. Santucci, Phys. Rev. B **35**, 5997 (1987).
[2] M. F. Roşu, F. Pleiter, and L. Niesen, Phys. Rev. B **63**, 165425 (2001).
[3] G. Boisvert and L. J. Lewis, Phys. Rev. B **56**, 7643 (1997).
[4] O. S. Trushin, P. Salo, and T. Ala-Nissila, Phys. Rev. B **62**, 1611 (2000).
[5] M. G. Del Pópolo, E. P. M. Leiva, and W. Schmickler, J. Electroanal. Chem. **518**, 84 (2002).
[6] J. A. Sprague, F. Montalenti, B. P. Uberuaga, J. D. Kress, and A. F. Voter, Phys. Rev. B **66**, 205415 (2002).
[7] T. Jacob, J. Anton, C. Sarpe-Tudoran, W.-D. Sepp, B. Fricke, and T. Baştuğ, Surf. Sci. **536**, 45 (2003).
[8] J. Frantz, M. Rusanen, K. Nordlund, and I. T. Koponen, J. Phys.: Condens. Matter **16**, 2995 (2004).
[9] O. Cheshnovsky, K. J. Taylor, J. Conceicao, and R. E. Smalley, Phys. Rev. Lett. **64**, 1785 (1990).
[10] S. Chen and J. M. Sommers, J. Phys. Chem. B **105**, 8816 (2001).
[11] H. Häkkinen, M. Moseler, O. Kostko, N. Morgner, M. A. Hoffmann, and B. Issendorff, Phys. Rev. Lett. **93**, 093401 (2004).
[12] A. Kudelski, J. Bukowska, M. Janik-Czachor, W. Grochala, A. Szummer, and M. Dolata, Vib. Spectrosc. **16**, 21 (1998).
[13] Ch. Loppacher, M. Bammerlin, M. Guggisberg, S. Schär, R. Bennewitz, A. Baratoff, E. Meyer, and H.-J. Güntherodt, Phys. Rev. B **62**, 16944 (2000).
[14] V. Zaporojtchenko, K. Behnke, T. Strunskus, and F. Faupel, Surf. Interface Anal. **30**, 439 (2000).
[15] F. Baumberger, T. Greber, and J. Osterwalder, Phys. Rev. B **62**, 15431 (2000).
[16] F. Reinert, G. Nicolay, S. Schmidt, D. Ehm, and S. Hüfner, Phys. Rev. B **63**, 115415 (2001).
[17] D. S. Martin, A. Maunder, and P. Weightman, Phys. Rev. B **63**, 155403 (2001).
[18] M. Hansmann, J. I. Pascual, G. Ceballos, H.-P. Rust, and K. Horn, Phys. Rev. B **67**, 121409(R) (2003).
[19] H. Haberland and B. v. Issendorff, Phys. Rev. Lett. **76**, 1445 (1996).
[20] A. Traverse, New J. Chem. **22**, 677 (1998).
[21] U. Busolt, E. Cottancin, H. Röhr, L. Socaciu, T. Leisner, and L. Wöste, Appl. Phys. B **68**, 453 (1999).
[22] H. Hövel, Appl. Phys. A **72**, 295 (2001).
[23] A. Fielicke, A. Kirilyuk, C. Ratsch, J. Behler, M. Scheffler, G. von Helden, and G. Meijer, Phys. Rev. Lett. **93**, 023401 (2004).
[24] F. Baletto and R. Ferrando, Rev. Mod. Phys. **77**, 371 (2005).
[25] C. Massobrio, A. Pasquarello, and A. Dal Corso, J. Chem. Phys. **109**, 6626 (1998).
[26] P. Calaminici, A. M. Köster, N. Russo, and D. R. Salahub, J. Chem. Phys. **105**, 9546 (1996).
[27] H. Åkeby, I. Panas, L. G. M. Pettersson, P. Siegbahn, and U. Wahlgren, J. Phys. Chem. **94**, 5471 (1990).
[28] M. Kabir, A. Mookerjee, R. Datta, A. Banerjea, and A. K. Bhattacharya, Int. J. Mod. Phys. B **17**, 10 (2003).
[29] H. Häkkinen, M. Moseler, and U. Landman, Phys. Rev. Lett. **89**, 033401 (2002).
[30] J. Olviedo and R. E. Palmer, J. Chem. Phys. **117**, 9548 (2002).
[31] J. Wang, G. Wang, and J. Zhao, Chem. Phys. Lett. **380**, 716 (2003).
[32] J. P. K. Doye and D. J. Wales, New J. Chem. **22**, 733 (1998).
[33] S. Darby, T. V. Mortimer-Jones, R. L. Johnston, and C. Roberts, J. Chem. Phys. **116**, 1536 (2002).
[34] M. W. Finnis and J. E. Sinclair, Philos. Mag. A **50**, 45 (1984), **53**, 161 (1986).
[35] J. García-Rodeja, C. Rey, L. J. Gallego, and J. A. Alonso, Phys. Rev. B **49**, 8495 (1994).
[36] C. Kuiying, L. Hongbo, L. Xiaoping, H. Qiyong, and H. Zhuangqi, J. Phys.: Condens. Matter **7**, 2379 (1995).
[37] S. Chantasiriwan and F. Milstein, Phys. Rev. B **53**, 14080 (1996).
[38] S. Chantasiriwan and F. Milstein, Phys. Rev. B **58**, 5996 (1998).
[39] L. García-González and J. M. Montejano-Carrizales, Phys. Status Solidi B **220**, 357 (2000).
[40] L. B. Hansen, P. Stoltze, J. K. Nørskov, B. S. Clausen, and W. Niemann, Phys. Rev. Lett. **64**, 3155 (1990).
[41] S. Valkealahti and M. Manninen, Phys. Rev. B **45**, 9459 (1992).
[42] O. B. Christensen and K. W. Jacobsen, J. Phys.: Condens. Matter **5**, 5591 (1993).
[43] E. E. Zhurkin and M. Hou, J. Phys.: Condens. Matter **12**, 6735 (2000).
[44] T. Zhang, A.-L. Wu, L. Guan, and Y.-H. Qi, Chin. J. Chem. **22**, 148 (2004).
[45] F. Baletto, R. Ferrando, A. Fortunelli, F. Montalenti, and C. Mottet, J. Chem. Phys. **116**, 3856 (2002).
[46] M. Kabir, A. Mookerjee, and A. K. Bhattacharya, Phys. Rev. A **69**, 043203 (2004).
[47] D. Schebarchov and S. C. Hendy, J. Chem. Phys. **123**, 104701 (2005).
[48] A. P. Sutton and J. Chen, Philos. Mag. Lett. **61**, 139 (1990).
[49] R. P. Gupta, Phys. Rev. B **23**, 6265 (1981).
[50] M. S. Daw and M. I. Baskes, Phys. Rev. Lett. **50**, 1285 (1983).
[51] M. S. Daw and M. I. Baskes, Phys. Rev. B **29**, 6443 (1984).
[52] S. M. Foiles, M. I. Baskes, and M. S. Daw, Phys. Rev. B **33**, 7983 (1986).
[53] A. F. Voter and S. P. Chen, in *Characterization of Defects in Materials*, edited by R. W. Siegal, J. R. Weertman, and R. Sinclair, MRS Symposia Proceedings No. 82 (Materials Research Society, Pittsburgh, 1987), p. 175.
[54] A. Voter, Los Alamos Unclassified Technical Report No LA-UR 93–3901 (1993).
[55] A. F. Voter, in *Intermetallic Compounds*, edited by J. H.

Westbrook and R. L. Fleischer (Wiley, New York, 1995), Vol. 1, p. 77.
[56] V. G. Grigoryan and M. Springborg, Phys. Rev. B **70**, 205415 (2004).
[57] V. G. Grigoryan and M. Springborg, Chem. Phys. Lett. **375**, 219 (2003).
[58] V. G. Grigoryan, D. Alamanova, and M. Springborg, Eur. Phys. J. D **34**, 187 (2005).
[59] http://www-wales.ch.cam.ac.uk/CCD.html
[60] W. H. Press, S. A. Teukolsky, W. T. Vetterling, and B. P. Flannery, in *Numerical Recipes in FORTRAN: the Art of Scientific Computing* (Cambridge University Press, Cambridge, 1992), p. 387.
[61] M. D. Morse, *Advances in Metal and Semiconductor Clusters, Vol. 1* (Spectroscopy and Dynamics), (JAI Press, Greenwich, CT, 1993), p. 83.
[62] V. A. Spasov, T. M. Lee, and K. M. Ervin, J. Chem. Phys. **112**, 1713 (2000).
[63] C. Mottet, G. Treglia, and B. Legrand, Surf. Sci. **383**, L719 (1997).